TESTING AND DESIGN OF BUCKLING RESTRAINED BRACES FOR CANADIAN APPLICATION

Tremblay, R.[1], Poncet, L.[2], Bolduc, P.[3], Neville, R.[4] and DeVall, R.[5]

SUMMARY

This paper presents qualifying tests performed on two Buckling Restrained Brace (BRB) members and describes an analytical study carried out to evaluate the seismic performance of structures equipped with these members. The test program examined the possibility of reducing the brace core length in order to increase brace axial stiffness. In the analytical study, the seismic performance of a 3-storey structure with buckling restrained braces is evaluated and compared to that of the same building designed with conventional steel braces. The results indicate that buckling restrained braced frames designed according to the 2005 National Building Code of Canada with an R_d factor of 4.0 would provide a level of performance comparable to that offered by Type MD concentrically braced steel frames. One main advantage of using buckling restrained braces is the reduction in the forces imposed on the foundations and surrounding structural elements.

INTRODUCTION

The use of Buckling Restrained Braced (BRB) frames in lieu of conventional concentrically braced steel frames (CBFs) is gaining popularity both for new construction or rehabilitation projects. BRB frames have the advantages of exhibiting a more stable hysteretic response and to impose reduced forces on the foundations and the adjacent structural elements that must be capacity protected. Compared to conventional tension-compression CBFs, the BRB system typically is laterally more flexible due to higher brace axial design stresses but this shortcoming can be overcome by reducing the length of the yielding core segment of the braces, L_c, to increase the brace axial stiffness, as shown in Fig. 1. Brace cores so designed are expected to experience higher strain demand, which could lead to premature fracture due to low-cycle fatigue under repeated inelastic cycles. Peak strains in the range of 1-2% are anticipated under severe ground motions and such amplitude has been considered in most test programs performed to date on BBR members (e.g., Watanabe et al. [1]; Saeki et al. [2]; Maeda et al. [3]; Ko et al. 2002 [4]). Recent tests by Iwata et al. [5], Tsai and Huang [6], and SIE [7] on braces made of structural steel grades used in

---

[1]Professor, [2]Research Associate, Dept. of Civil, Geological and Mining Eng., Ecole Polytechnique, P.O. Box 6079, St. Centre-ville, Montreal, Canada H3C 3A7
[3]Graduate Research Assistant, Dept. of Civil Eng., Laval University, Quebec, Canada, G1K 7P4.
[4]Associate, [5]Principal, Read Jones Christoffersen, 1285 West Broadway, Vancouver, Canada V6H 1X8

Japan indicate that such braces can sustain loading histories with strains in the range of up to 3-6%, as anticipated under near-field earthquake events.
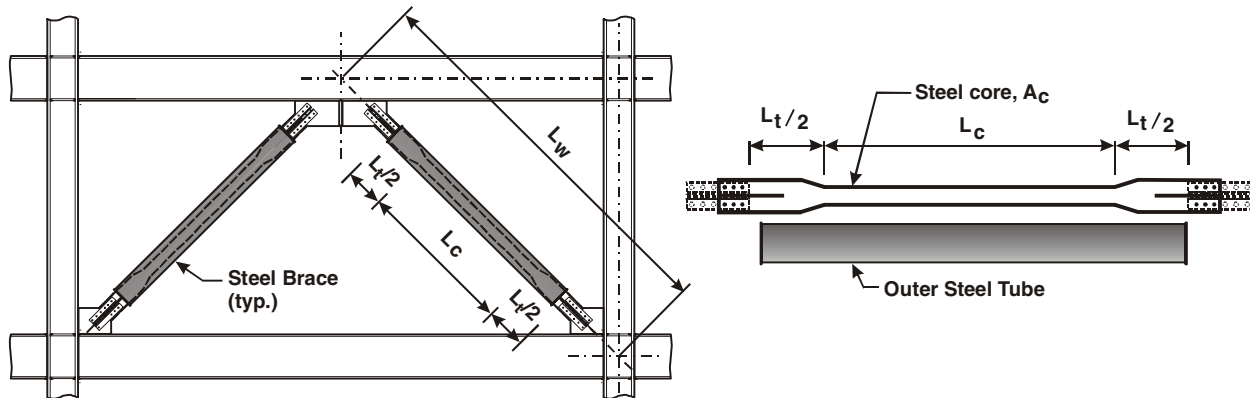
Figure 1: Typical buckling restrained braced frame and buckling restrained brace.

The first part of the paper summarizes the findings of a sub-assemblage test program that was conducted on concrete filled tube buckling restrained braces to assess their potential to withstand high seismic induced strain demand when fabricated with structural steel currently in use in Canada. In the second part of the paper, an analytical study is carried out to examine the seismic performance of adjacent three-storey building structures constructed with three different braced frame systems: buckling restrained braces with long and short core segments, respectively, and a tension-compression conventional CBF system. The structures are located in Vancouver, B.C. and are designed according to the seismic provisions of the upcoming 2005 edition of the National Building Code of Canada (NBCC) (Heidebrecht [8]). Design aspects such as the prediction of the strain demand on brace cores in the BRB frames and the design forces to be considered for the foundations are discussed. Peak storey drifts, minimum building separation, inelastic demand on brace elements, and peak forces that develop in the foundations are examined for each system. Modeling techniques for buckling restrained braces are also discussed.

TEST PROGRAM

Test specimens
Sub-assemblage testing of buckling restrained braces was performed in a 4.877 m width x 3.658 m tall steel frame mounted horizontally in the Structural Engineering Laboratory at Ecole Polytechnique of Montreal (Fig. 2). The test frame was truly pinned at its four corners and the load was applied by means of a 1.5 MN actuator. The experimental program included two brace specimens that were each composed of a steel core element inserted in a cold formed (Type C) circular HSS 273x6.4 tube made of G40.21-350W steel filled with 20 MPa flowable pea gravel concrete. The core was made of G40.21-350WT steel with enhanced thoughness properties. The measured yield and tensile properties of the core steel material were F_y = 370 MPa and F_u = 492 MPa, and the core cross-section was 12.7 mm x 125 mm, resulting in a brace yield load, P_y, of 587 kN. The only difference between the two braces was the length of the core segment: L_c = 2483 (Specimen C1-1) and 1001 mm (Specimen C2-1).

The brace ends were stiffened to ensure stable elastic response outside of the tube, and the connections to the test frame were done with high-strength bolts and splice plates (see Fig. 2). The stiffeners extended a minimum of 256 mm into the tubes. The core plates were flame cut from single plate elements (no splices permitted) using a numerically controlled equipment. Transitions between the core and the end segments were sloped at 1:4 with 102 mm radius. The edges of the core and transition segments were ground to

achieve a smooth finish with no visible notching. After fabrication of the core plates, trapezoidal 12.7 mm thick blocks made of flexible (Styrofoam) material were placed against the interior edges of the core end stiffeners as well as against the interior side of the transition zones to allow the brace cores to deform freely in compression without direct bearing against the concrete fill. A 3 mm thick flexible material (Dow Ethafoam 222) was placed on both edges of the plates along the middle core segment to permit lateral expansion of the core due to Poisson's effects. The brace plates were then wrapped with 4 layers of 0.2 mm polyethylene film secured with tape to break the bond between the concrete and the core.

Figure 2: Brace specimen in the test frame.

Test protocol

The qualifying quasi-static cyclic test sequence that was considered at the time of testing for inclusion in future NEHRP provisions for Buckling Restrained Braces was adopted for the test program (Sabelli [9]). This test protocol starts with 6 cycles at $\Delta = \Delta_y$ and the amplitudes in the subsequent cycles are based on the design storey drift, Δ_m, for the frame studied: 4 cycles at $\pm 0.5 \Delta_m$, 4 cycles at $\pm 1.0 \Delta_m$, and 2 cycles at $\pm 1.5 \Delta_m$. In the NEHRP draft provisions, the value of Δ_m must not be taken lower than 0.01 h_s but need not exceed 5.0 Δ_y. For buildings of the normal importance category designed according to the 2005 NBCC, it is expected that the anticipated total storey drift, including inelastic deformations, be equal to or greater than 5.0 Δ_y and, therefore, $\Delta_m = 5.0 \Delta_y$ was adopted for the test sequence. Under the large amplitude cycles at $\pm 7.5 \Delta_y$ (1.5 Δ_m), the maximum strain demand on the brace cores were expected to reach respectively 1.9% and 3.7% for the long and short brace core specimens.

Test results

Both specimens could withstand the total displacement history and it was decided to apply four extra cycles with displacements varying from 0 to +10.0 Δ_y (+ = tension in the brace) to assess the reserve in fracture life. Figure 3 shows the measured brace axial load-core strain relationship for both specimens, the brace load P being obtained assuming truss response of the system and normalized to the yield load $P_y = 587$ kN. Table 1 gives the normalized peak storey shear in the frame, V/V_y, as measured in the first and second cycles at each displacement level (V+ induce tension in the brace specimen). During the six elastic cycles, the lateral stiffness of the frame was determined from measurements and compared to theoretical predictions. The test-to-predicted ratios are equal to 1.00 and 1.04 for Specimens C1-1 and C2-1, respectively, indicating that the method that was used, and which is discussed later in the next section, can be employed to accurately evaluate the lateral stiffness of BRB frames.

The plots in Fig. 3 show that both specimens exhibited a stable and repeatable response with steadily increasing resistance over the entire qualifying test protocol and the four additional tension loading cycles.

No damage could be observed except small concrete debris coming out of the tube end plates during the additional tension displacement cycles at 10 Δ_y. After the first inelastic excursion at -2.5Δ_y, the transition from elastic to inelastic behavior became more progressive due to the Baushinger effect on the steel core. The transition is smoother on the compression side, probably because the core developed limited local buckling prior to yielding due to the clearance left between the core and the concrete fill. As larger deformation amplitudes and further cycles were applied, both kinematic and isotropic strain hardening responses in the steel core material resulted in a gradual increase of the brace resistance upon yielding. The brace stiffness in the inelastic range is generally higher in compression, and the difference is more pronounced towards the end of the large 5.0 Δ_y and 7.5 Δ_y compression excursions. The second slope in tension can be mainly attributed to strain hardening whereas friction developing between the locally buckled steel core and the buckling restraining mechanism likely also contributed to the increase in strength upon yielding in compression. Frictional response between the core and the concrete fill is supported by strain gauge readings on the steel tube which indicate that axial compression developed in the tube when approaching peak maximum compression displacements, immediately followed by tube tension forces when the imposed displacement was reversed. In Test C2-1, slippage of one of the end bolted connections occurred in tension and compression during the last two cycles at 7.5 Δ_y, which produced the sudden drops in capacity that can be noticed in Fig. 3b. However, that phenomenon had no consequences on the brace response.
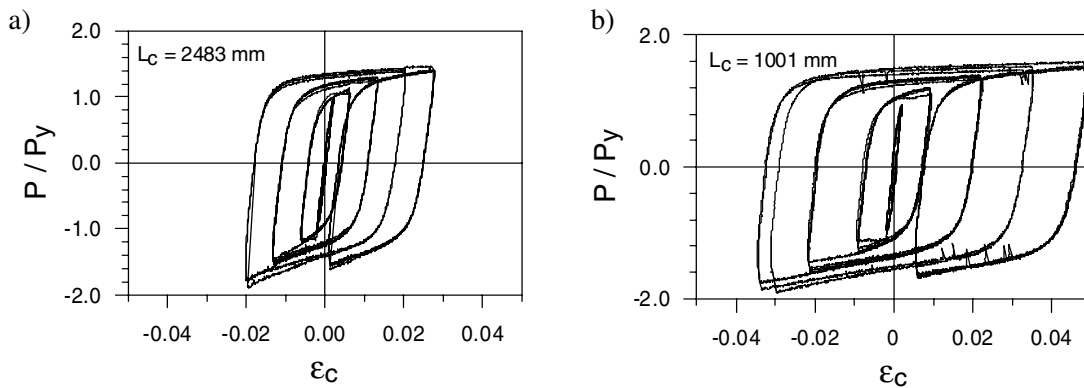
Figure 3: Measured axial load-core deformation in Tests: a) C1-1; b) C2-1.

Table 1: Measured peak loads in first two cycles at each deformation amplitude

Cycle	Specimen C1-1				Specimen C2-1			
	$\varepsilon_c -$ (%)	V/V_y ( )	$\varepsilon_c +$ (%)	V/V_y ( )	$\varepsilon_c -$ (%)	V/V_y ( )	$\varepsilon_c +$ (%)	V/V_y ( )
1	-0.19	-1.00	0.20	0.99	-0.18	-1.00	0.19	0.95
2	-0.20	-1.05	0.21	0.94	-0.19	-1.01	0.20	0.94
7	-0.61	-1.18	0.62	1.06	-0.92	-1.13	0.92	1.11
8	-0.61	-1.18	0.62	1.06	-0.92	-1.25	0.94	1.18
11	-1.3	-1.46	1.3	1.25	-2.1	-1.44	2.2	1.34
12	-1.3	-1.52	1.3	1.29	-2.1	-1.54	2.2	1.37
15	-2.0	-1.77	2.0	1.39	-3.3	-1.75	3.5	1.47
16	-2.0	-1.78	2.0	1.42	-3.4	-1.88	3.3	1.52
17	-	-	2.7	1.45	-	-	4.5	1.60
18	-	-	2.7	1.41	-	-	4.8	1.54

In Table 1, the measured peak loads with the brace acting in tension in the first cycles are slightly less than P_y, in both tests, even if ε_c reached ε_y of the steel material ($\varepsilon_y = 0.185\%$). This is due to the gradual transition between elastic and yielding responses, after inelasticity had developed in previous cycles (cycles started with compression). In the subsequent cycles at larger amplitude, the peak tension loads amplified to eventually reach forces corresponding to the attainment of the steel tensile stress ($F_u / F_y = 1.33$) at peak core strains of approximately 2%. Under larger positive deformations, the apparent core stress exceeded F_u, probably as a result of small secondary forces developing in the test frame at large deformations. In compression, the peak applied load reached approximately 1.5 V_y in the cycles at $\Delta_m = 5.0 \Delta_y$ (Cycles nos. 11 and 12) and 1.8 V_y in the cycles at 7.5 Δ_y. As indicated earlier, such larger forces in compression are the consequence of the friction between the core and the concrete, and the composite action of the exterior tube and the concrete fill. In tension, similar tension loads were observed at similar strain levels for the two specimens. Conversely, in compression, the peak compression forces seem to be dependant upon the number of cycles, rather than the core strain amplitude, as both specimens developed the same brace loads in the same cycles during the tests.

ANALYTICAL STUDY

Buildings studied

The influence of specifying different brace core lengths on the seismic performance of BRB frames is examined through nonlinear dynamic analysis of a hypothetical 3-storey building located in Vancouver, B.C., along the Pacific west coast of Canada (Fig. 4). The structure comprised a 13970 sq. m storage area and a 7010 sq. m. retail area. Both structures are separated by a construction joint and behave individually. Gravity loads are given in the figure. The design floor live load is the same for both structures except that 100% of that load must be considered as acting concomitantly with the seismic loads for the storage area, which results in larger seismic weight and higher P-delta effects than in the retail area where 50% of the live loads is combined with earthquake effects.
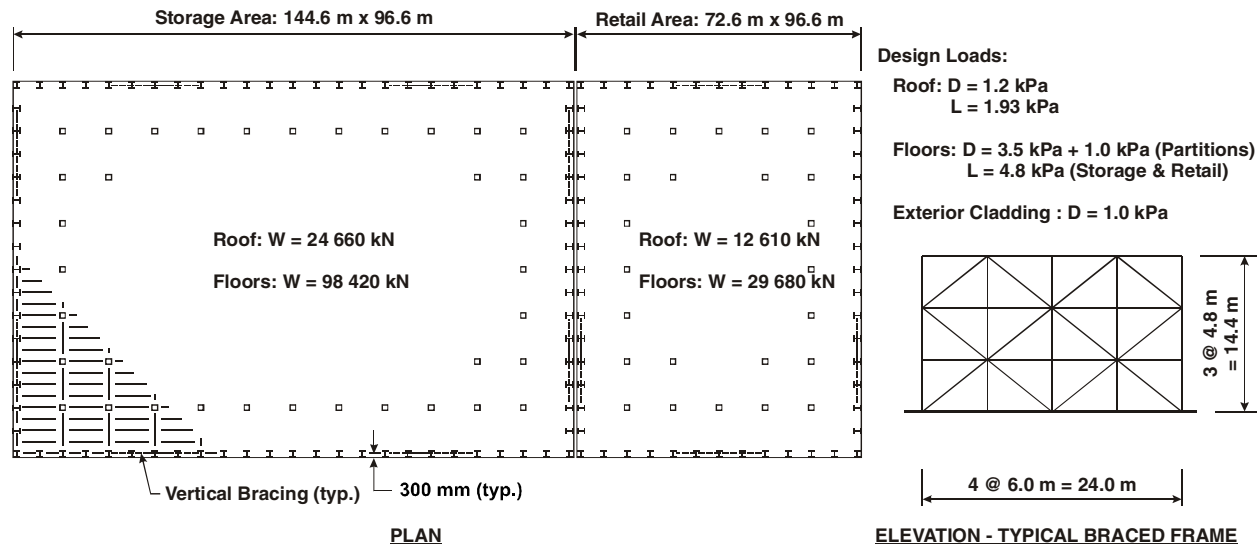
Figure 4: Buildings studied.

In each principal direction, the seismic force resisting system of the storage building consisted of four 24 m, 4-bay long concentrically braced steel frames located along the exterior walls. Two such bracing bents were used in each orthogonal direction for the retail building. Rigid diaphragm behavior was assumed and structural steel with $F_y = 345$ MPa was used throughout. Three different bracing members were considered: buckling restrained braces with long core segments (BRB-L), buckling restrained braces with

short core segments (BRB-S), and conventional tension-compression braces (CBF system). The latter was included for comparison purposes and the braces were assumed to be made of square HSS sections acting in tension and compression. The center-to-center dimension of the braces, L_w, was equal to 7684 mm and it was assumed that the total transition zone, L_t (see Fig. 1), would be 500 mm long and that the connections would require a minimum length of 1300 mm, thus leading to a maximum core length, L_c of 5884 mm for the BRB-L system. For the BRB-S frame, the core segment dimension was reduced to 1300 mm and L_t was increased to 5084 mm, as discussed next. Note that the same core length was used for the two buildings as would typically be the case in practice. For modeling the structures, the BRB members were considered as bar elements with equivalent cross-sectional area, A_e, given by (Chen et al. [11]):

$$[1] \qquad A_e = \frac{L_w}{\dfrac{L_c}{A_c} + \dfrac{L_t}{A_t} + \dfrac{L_j}{A_j}} = \frac{A_c L_w}{L_c + L_t \dfrac{A_c}{A_t} + L_j \dfrac{A_c}{A_j}}$$

The ratios $A_c/A_j = 0.3$ and $A_c/A_t = 0.5$ were assumed for both structures (A_j and A_t = cross-sectional area of the joint and transition portions of the braces, respectively). This resulted in $A_e/A_c = 1.18$ and 1.82 for the long and short brace core lengths, respectively.

Design of the braced frames
The design of the structure was performed according to the 2005 NBCC and the CSA-S16 Standard for the design of steel structures [12]. The seismic loads were determined according to the static equivalent force procedure with the lateral force at the base of the structure, V, given by:

$$[2] \qquad V = S(T_a)\, M_v\, I_E\, W / (R_o\, R_d) < (2/3)\, S(0.2)\, I_E\, W / (R_o\, R_d)$$

where $S(T_a)$ is the design response spectral acceleration at the design fundamental period, T_a, taken as $F_a S_a(0.2)$ for $T_a < 0.2$ s, the smaller of $F_v S_a(0.5)$ and $F_a S_a(0.2)$ at $T_a = 0.5$ s, $F_v S_a(1.0)$ at $T = 1.0$ s, and $F_v S_a(2.0)$ at $T = 2.0$ s. For periods between 0.2 and 2.0 s, S is obtained by linear interpolation. In these expressions, F_a and F_v are respectively the acceleration-based and velocity-based site coefficients and the values of $S_a(T_a)$ correspond to 2% in 50 years uniform hazard spectral (UHS) acceleration ordinates specified for the site. M_v is a factor that accounts for higher mode effects on base shear, I_E is the importance factor, W is the seismic weight, and R_d and R_o are respectively the ductility- and overstrength-related force modifications factors of the structural system. For braced steel frames, T_a can be taken as $T_a = 0.025\, h_n$, where h_n is the building height (in m). Alternatively, the period obtained from methods of mechanics can be used provided that it does not exceed two times the value given by the empirical expression. The second approach was used herein and T_a was therefore limited to 0.72 s ($h_n = 14.4$ m). For Vancouver, S_a values of 0.96, 0.66, 0.34, and 0.18 g were used at $T = 0.2, 0.5, 1.0,$ and 2.0 s, respectively. Firm ground condition (Site Class C) was assumed in the study, with $F_a = F_v = 1.0$. For these structures, the M_v factor was equal to 1.0 and the buildings were of the normal importance category with $I_E = 1.0$. The seismic weight values at each level are given in Fig. 4 for both buildings.

For the CBF system, Type MD (Moderately Ductile) braced steel frames were adopted, which classify for $R_d = 3.0$ and $R_o = 1.3$. In the proposed NBCC 2005, values have not yet been adopted for R_d and R_o for BRB frames. In view of the anticipated similitude in inelastic response between the BRB system and Ductile Eccentrically Braced Steel Frames (EBFs), the value $R_d = 4.0$ specified for EBFs was tentatively retained herein for the design of the BRB frames. The overstrength-related factor, R_o, accounts for the dependable overstrength that can be mobilized in a structure. It can be obtained from (Mitchell et al. [13]) $R_o = R_{size}\, R_\phi\, R_{yield}\, R_{sh}\, R_{mech,}$ where R_{size} is the overstrength arising from restricted choices for sizes of

members and elements and rounding of sizes and dimensions, R_ϕ is a factor accounting for the difference between nominal and factored resistances, R_{yield} is the ratio of actual yield strength to minimum specified yield strength, R_{sh} is the overstrength due to the development of strain hardening, and R_{mech} is the overstrength arising from mobilizing the full capacity of the structure such that a collapse mechanism is formed. In order to minimize concentration of inelastic demand along the building height, it is expected that the cross-section area of the brace fuse segment will typically be adjusted at every floor so that its factored resistance closely matches the factored code force level. Hence, it is advisable to use $R_{size} = 1.0$ for Buckling Restrained Braced Frames. The factors R_ϕ and R_{yield} are respectively equal to 1.11 (= $1/\phi$) and 1.10 for steel (Mitchell et al. 2003). R_{sh} accounts for the ability of strain hardening to develop in the material at the anticipated level of deformation for the structure studied. A review of past experimental studies on Buckling Restrained Braces suggests that a value of 1.10 is suitable for this parameter. A value of 1.0 is chosen for R_{mech}, as a full mechanism rapidly develops after initiation of yielding in the braces. Substituting all these values gives $R_o = 1.34$, and a conservative value of 1.3 was selected for this study.

Table 2 presents the key seismic design parameters and the main characteristics of the three braced frames. For the BRB structures, the calculated fundamental periods were longer than the upper limit for T_a (0.72 s), even when the short core segments were specified, and that period was used to determine the seismic loads. The BRB frames with the long core braces thus possessed approximately 30% extra lateral capacity compared to the short core system due to the differences between design and actual periods: S (0.90 s) / S(0.72 s) = 1.30. For the CBF system, braces were designed for compression assuming an effective length factor of 0.9. This resulted in stiffer structures with shorter periods which, when combined to the higher R_d factor, resulted in design seismic loads (V/W) approximately 60% larger than for the BRB frames. Note that in design T_a was determined with simplified analytical method, which explains the slight difference between T_a and T_1 at the bottom of the table, the latter being determined with eigenvalue analysis after completion of the design. Brace forces due to gravity loads were considered in the brace design and the selected brace dimensions are given in Table 2. For the CBF system, the brace slenderness varied between 59 and 103 for the storage building and between 70 and 101 for the retail area.

Table 2: Building properties and design parameters

Parameter	BRB-L		BRB-S		CBF	
	Storage	Retail	Storage	Retail	Storage	Retail
T_a (s)	0.72	0.72	0.72	0.72	0.57	0.56
V/W	0.10	0.10	0.10	0.10	0.16	0.16
Brace 3	PL13x143	PL13x120	PL13x143	PL13x120	HSS178x13	HSS178x10
Brace 2	PL19x246	PL19x161	PL19x246	PL19x161	HSS254x13	HSS203x13
Brace 1	PL25x253	PL25x159	PL25x253	PL25x159	HSS254x16	HSS254x13
Δ_3/h_s (%)	1.20	1.26	0.82	0.85	0.39	0.46
Δ_2/h_s (%)	1.40	1.42	0.95	0.96	0.68	0.61
Δ_1/h_s (%)	1.25	1.29	0.80	0.84	0.67	0.66
Δ_{sep}/h_n (%)	1.84		1.23		0.82	
ε_{c3} (%)	0.66	0.70	1.52	1.65	-	-
ε_{c2} (%)	0.79	0.82	1.92	2.00	-	-
ε_{c1} (%)	0.77	0.80	1.86	1.95	-	-
T_1 (s)	0.89	0.92	0.73	0.76	0.58	0.58
T_2 (s)	0.34	0.41	0.32	0.33	0.24	0.24

In NBCC 2005, lateral deformations under the design seismic load must be multiplied by R_oR_d/I_E to give realistic estimates of the anticipated deflections, including inelastic response effects. For buildings of the normal importance category ($I_E = 1.0$), storey drifts so computed must be limited to 0.025 h_s. The total anticipated storey drifts, as normalized with respect to storey height h_s, are given in Table 2. The limit is met in all cases. Reducing L_c from 5884 mm to 1300 mm permitted to reduce the deflections of the BRB frames by approximately 30%. However, the anticipated drifts for the CBF system remained lower than such reduced values. In the 2005 NBCC, the minimum separation between adjacent structures, Δ_{sep}, is equal to the square root of the sum of the squares of the individual anticipated deflections determined for each building. This calculation was performed for each of the systems and the required Δ_{sep} at the roof level is given in Table 2. Again, the required net distance is smaller for the CBF system. For the BRB members, the peak strain demand on the brace cores, ε_c, is determined from the anticipated total elongation of the equivalent brace, δ_e ($= R_dR_o/I_e$ times the brace deformation under design seismic loads):

$$[3] \qquad \varepsilon_c = \left[\delta_e - P\left(\frac{1}{K_e} - \frac{1}{K_c}\right)\right]\frac{1}{L_c}$$

, where P is the anticipated brace load at maximum deformation, $K_e = EA_e/L_w$, and $K_c = EA_c/L_c$. The second term in brackets corresponds to the brace elastic deformation outside of the core segment and P is taken as equal to $A_cR_{yield}R_{sh}F_y$ in this calculation. The stiffness ratios $K_e/K_c = 0.90$ and 0.31 for $L_c = 5884$ and 1300 mm, respectively. As indicated, peak strains in short core braces are approximately 2.4 times higher than those predicted in the long core braces, in spite of the fact that they result from smaller storey drifts. The length of the short brace core was adjusted to limit the strain demand to 2%.
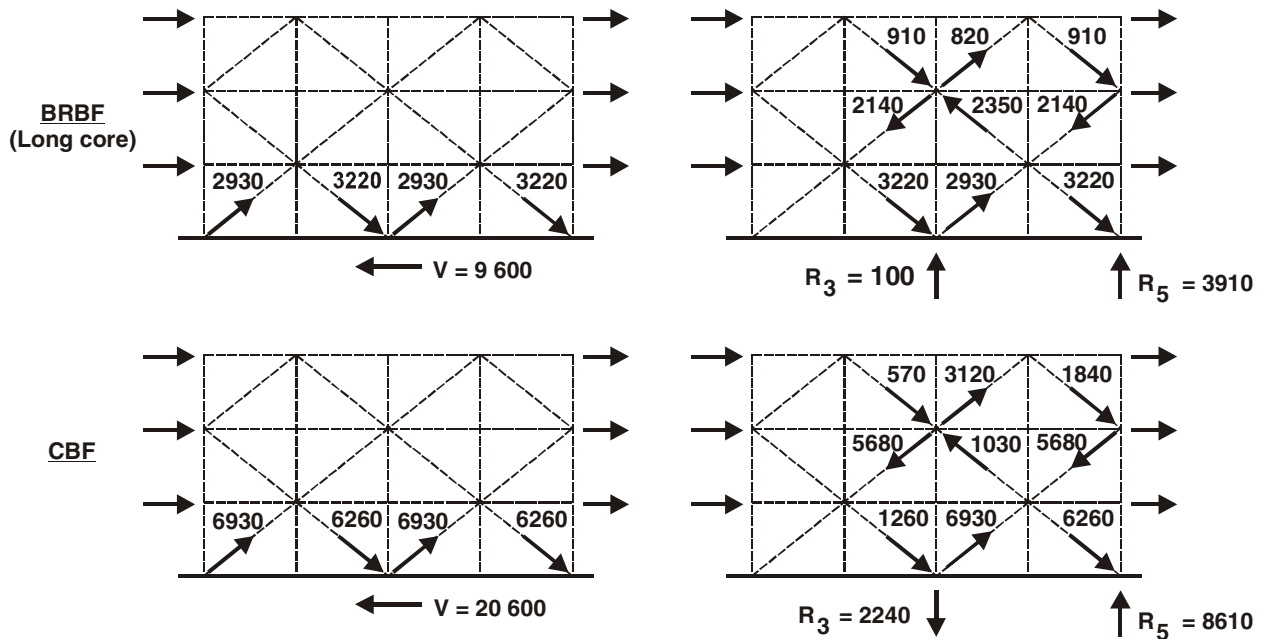
Figure 5: Calculation of maximum expected base shear and vertical reactions R_3 and R_5 (in kN)

Figure 5 illustrates partial capacity design calculations that would be performed for the design of the foundations of the storage building. Only the base shear and the vertical reactions at the center and at the edge of the bracing bents are shown. For both systems, the braces are replaced by the forces that would be delivered by these elements upon inelastic response. For the BRB frame, the values are determined from

the test results and the anticipated strain levels for $L_c = 5884$ mm. The peak tension load was determined using an axial core stress of 1.2 $R_{yield}F_y$, the factor 1.2 representing strain hardening at strains of up to 1%, as per Table 1. In compression, the brace design load was increased by an additional 10% to account for friction between the core and the buckling restraining mechanism. For the CBF system, the maximum brace tension load is based on a stress equal to 1.1 $R_{yield}F_y$, the factor 1.1 being added to CSA-S16 requirements to account for strain hardening (Tremblay [14]). For compression, the resistance at first buckling (= 1.2 times the unfactored resistance with $R_{yield}F_y$) is used for the base shear and the reaction R_5. For R_3, the post-buckling brace strength, taken equal to 0.2$AR_{yield}F_y$ is used, as it produces higher compression in the central column. In design, gravity load effects must be added to the forces shown. These simple calculations clearly show that significant cost savings can be achieved by adopting BRB frames, the induced reactions for this system being much lower than for the conventional CBF design.

Analytical modeling
Nonlinear dynamic analyses of the three building designs were performed to examine their seismic performance. In addition, for the BRB frames, two sets of analyses were carried out with two different brace hysteretic models to examine the influence of modeling assumptions. In all cases, a 2D analytical model was used that included one bracing bent of the storage building and one bracing bent of the retail building, arranged side by side. Each bracing bent was assigned its tributary seismic mass, excluding accidental torsional effects. The model also included all gravity columns being laterally braced by each bracing bent. For each braced frame and its tributary gravity columns, the nodes at a given floor were constrained to experience the same horizontal displacements, assuming rigid diaphragm response. All columns were of the same cross-section and continuous over the building height. A constant acceleration integration scheme with constant time step of 0.0005 s was adopted. P-delta effects were included with concomitant gravity loads of D + 1.0 L for the storage building and D + 0.5 L for the retail area. Rayleigh damping with 3% critical damping in modes 1 and 4 of the 2-building model was considered.

The analysis of the buckling restrained braced frames was performed with the Ruaumoko computer program (Carr [15]). The first brace hysteretic model is a symmetrical Ramberg-Osgood formulation that was modified to prevent off-sets of the forces in small amplitude cycles (Pyke model) and to include the isotropic/kinematic (I-K) strain hardening model proposed by Nakashima et al. [16]. The Ramberg-Osgood multiplier, α, was set equal to 1.0 for all braces. The weighting coefficient, β, and the Ramberg-Osgood factor, r, were adjusted to match the results from Tests C1-1 and C2-1. Figure 6a shows the correlation between hysteretic models adopted for the long and short core braces at the first storey of the retail building and Test C1-1. In these comparisons, test results are modified as follows: the test brace loads P/P_y in Fig. 3 are multiplied by the model brace yield load whereas the deformations δ_e are back calculated from Equation [3] using the history of core strains ε_c applied in the test, the corresponding brace load as transformed for the model brace, and the stiffness properties of the model brace. In tension, the brace yield load was based on the expected yield strength $R_{yield}F_y = 380$ MPa. In compression, the yield load was increased further by 10% to account for friction response. As shown, this resulted in a good match, on average, over most of the hysteresis cycles. Only the large increases in compression loads at large negative deformations could not be reproduced adequately with the model. Figure 6b shows the same correlations for the second hysteretic model exhibiting bi-linear response. For this model, the tension yield capacity was also set with the expected yield strength and the 10% increase in compression was also specified. The bi-linear factors, r_e, were determined for the long and short core braces using:

$$[4] \qquad r_e = \frac{P - P_y}{\left(\delta_e - \delta_{ye}\right) K_e} = \frac{P/P_y - 1}{\dfrac{\varepsilon_c L_c}{\delta_{ye}} + \left(\dfrac{P}{P_y}\right)\left(1 - \dfrac{K_e}{K_c}\right) - 1}$$

In this equation, δ_{ye} is the deformation at yield for the equivalent brace element (= P_y/K_e), and the r_e values were set such that P/P_y reached a value of 1.3 at a core strain of 2%, as observed in tension in the tests (Table 1). This is confirmed in Fig. 6b by the good match in capacity between the test and the model at maximum positive deformation attained in Test C1-1. As shown, this simple bi-linear representation underestimates the actual brace capacity in the small deformation range, and the large increases in brace compression resistance could not be captured either by the model.
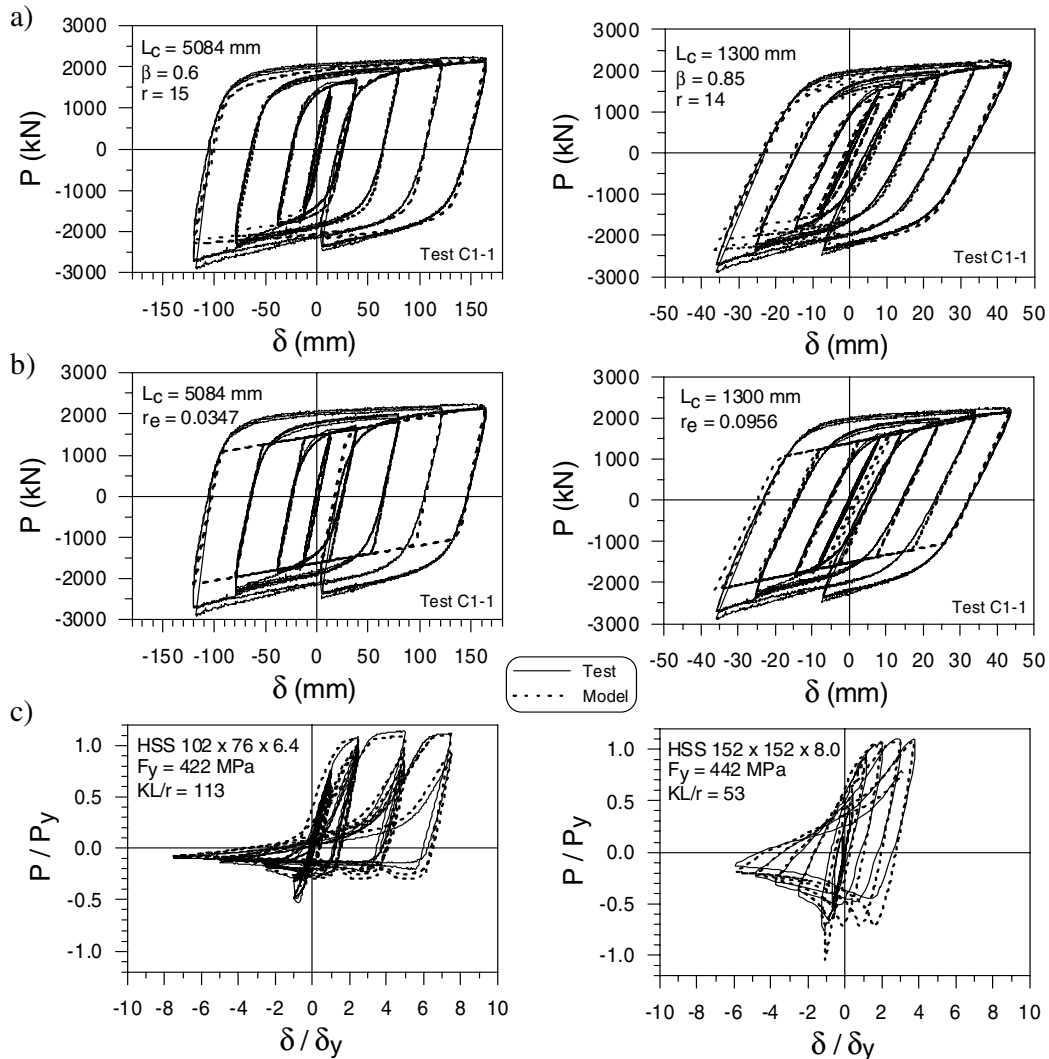
Figure 6: Brace models: a) I-K Ramberg-Osgood model of Level 1 braces in the retail building; b) Bi-linear model of Level 1 braces in the retail building; c) Calibration of the Ikeda brace model against test data for two brace slenderness ratios.

For the CBF structures, the Drain-2DX computer program [17] was used with the physical hysteretic brace model by Ikeda and Mahin [18]. The parameters of the brace models were adjusted to obtain a good correlation with past test results obtained for two braces having the maximum and the minimum slenderness used in the buildings. The correlation is shown in Fig. 6c for these two braces. The measured tension capacity upon yielding could be reproduced adequately specifying 1.05 times the steel yield strength measured in the tests and by using 2% strain hardening. In the building models, the brace yield strength was therefore determined with $1.05R_{yield}F_y$. An effective length factor of 0.9 was also specified.

The structures were subjected to an earthquake record ensemble that included four simulated and six historical ground motion time histories produced by intra-plate seismic events matching the two dominant magnitude-hypocentral distance scenarios for the Vancouver region: $\mathbf{M}$6.5 at 30 km and $\mathbf{M}$7.2 at 70 km. This ground motion ensemble is described in [19].

Analysis results
Building performance
Table 3 presents the mean + one standard deviation (M+SD) values of the peak storey drifts at each level, peak core strains at each level, peak roof lateral deformations, and peak relative roof deformations (Δ_{sep}). Values in brackets are for the bi-linear BRB brace model and will be discussed later.

Table 3: Mean+SD value of peak response parameters

	BRB-L		BRB-S		CBF	
Parameter	Storage	Retail	Storage	Retail	Storage	Retail
Δ_3/h_s (%)	0.86 (0.92)	1.04 (1.11)	0.74 (0.63)	0.79 (0.67)	0.37	0.62
Δ_2/h_s (%)	1.38 (1.25)	1.50 (1.24)	0.96 (0.92)	0.93 (0.88)	0.70	1.39
Δ_1/h_s (%)	1.97 (1.59)	2.15 (1.69)	1.61 (1.37)	1.67 (1.39)	1.44	0.94
ε_{c3} (%)	0.53 (0.57)	0.64 (0.69)	1.72 (1.27)	1.81 (1.38)	-	-
ε_{c2} (%)	0.87 (0.78)	0.95 (0.78)	2.33 (2.09)	2.22 (1.99)	-	-
ε_{c1} (%)	1.27 (1.01)	1.37 (1.07)	4.21 (3.36)	4.40 (3.41)	-	-
Δ_{roof}/h_n	1.29 (1.01)	1.43 (1.11)	0.88 (0.81)	0.91 (0.83)	0.63	0.73
Δ_{sep}/h_n	0.33 (0.36)		0.23 (0.19)		0.42	

Table 4: Peak roof drift angle to first storey drift angle ratios

	BRB-L		BRB-S		CBF	
Parameter	Storage	Retail	Storage	Retail	Storage	Retail
$(\Delta_{roof}/h_n)/(\Delta_1/h_s)$						
Mean	1.52	1.43	1.63	1.75	1.87	1.42
Maximum	2.29	2.13	2.35	2.27	2.70	2.13
Roof drift ratio						
Mean	0.32	0.32	0.26	0.25	0.24	0.23
Maximum	0.77	0.78	0.57	0.57	0.44	0.50

The peak storey drifts for all systems are less than the 2.5% h_s code limit. On average, the storey drifts obtained for the BRB frames do correspond to the anticipated values, but larger storey drifts, in excess of the anticipated $R_dR_o\Delta$ values, developed at the first floor while the demand at the topmost floor was lower than expected. The same trends are observed for the CBF system. For the CBF retail building, large storey drift (2.6% h_s) developed at the 2nd floor under a single record, leading to the higher M+SD value in Table 3. Table 4 presents statistics of the ratio of the peak roof drift angle (Δ_{roof}/h_n) to the peak storey drift angle at first floor (Δ_1/h_s). As shown, the mean values are typically above 1.5 with maximum values well in excess of 2.0, confirming the concentration of inelastic demand in the bottom floor. The phenomenon appears to be relatively more pronounced for the BRB frames with shorter core length and the CBF structures. Core strains in BRB members follow the same trends with M+SD values at Level 1 typically 1.5 and 2.2 times greater than the predictions for the long and short brace cores, respectively. For the shorter core braces, that concentration is more pronounced than expected from storey drift results. This is because core strains increase at a higher rate than storey drifts when a shortened brace core segment is

used. Variations in storey drifts then produce amplified variations in core strain values, which suggests that plastic demand in short core braces is more sensitive to scatter in results and, thus more difficult to predict with accuracy. Table 3 also shows that the building separation required between adjacent BRB frames with nearly same vibration periods is less than 20% of the NBCC specifications (Table 2). Reducing brace core length had a positive impact on that parameter. For the CBF system, the M+SD building separation is approximately 50% of the NBCC recommended value.
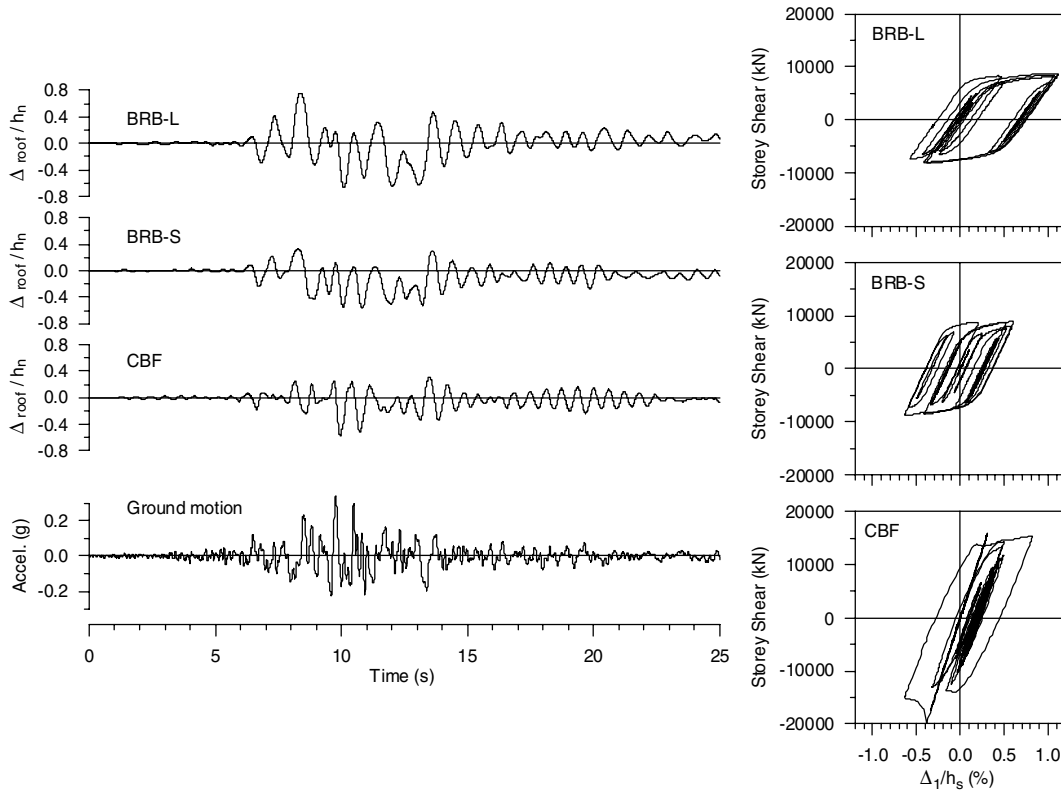
Figure 7: Roof drift time histories and first storey V-Δ response under Record No. 8

Table 4 also gives the mean and the maximum values of the roof drift ratio computed for each bracing system. That roof drift ratio is equal to the difference between peak roof displacement values in opposite directions divided by the sum of the peak roof drift values in opposite directions. Calculations are done with absolute deformation values in both directions, such that a ratio equal to 0 indicates perfectly symmetrical response and 1.0 is obtained for deformations developing only towards one direction. As shown, reducing the length of the core for the BRB frames seems to improve the symmetry of the response, but not to the level achieved with conventional CBF construction. Close examination of the time history results reveals that the response of the structures can be grouped into two categories: mainly symmetrical and significantly unsymmetrical, depending essentially upon the ground motion signature. One example of each type is shown in Figs. 7 and 8. In the first category, the building oscillates about the undeformed position whereas the response in the second group includes a large displacement towards one direction, the latter being typically the result of an acceleration pulse in the ground motion (Fig. 8). As illustrated in the figures, reduced BRB core lengths is more effective for the first response type, suggesting that short core braces would have limited benefits in near-fault applications. CBFs have larger lateral capacity, resulting in lower inelastic demand and less vulnerability against impulsive input. In addition, for the more slender braces, the difference between tension and compression resistances can create significant back-up capacity by the tension braces, which helps in limiting inelastic deformations.
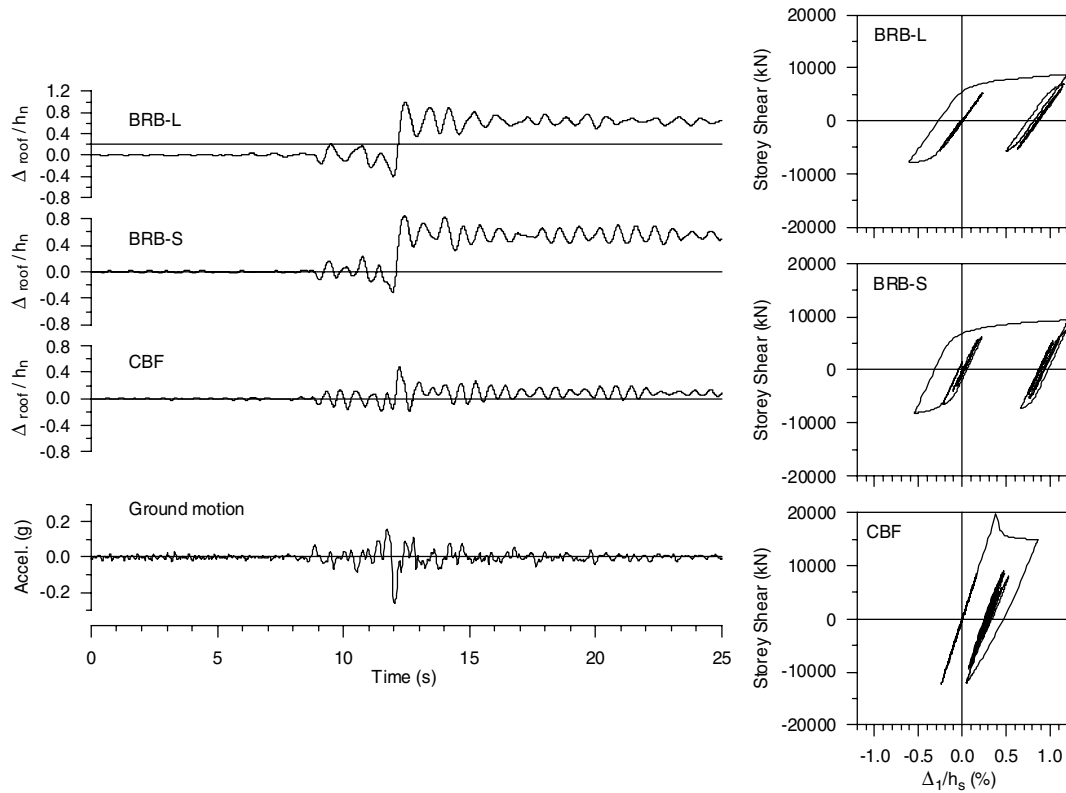
Figure 8: Roof drift time histories and first storey V-Δ response under Record No. 9

Table 5: 84th percentile of peak force response parameters

	BRB-L		BRB-S		CBF	
Parameter	Storage	Retail	Storage	Retail	Storage	Retail
$P / P_{y, 3}$	0.97 (1.06)	0.99(1.07)	0.93 (1.19)	0.99 (1.20)	0.72	0.87
$P / P_{y, 2}$	1.03 (1.09)	1.01(1.09)	1.10 (1.30)	1.08 (1.25)	1.05	1.05
$P / P_{y, 1}$	1.07 (1.11)	1.04(1.13)	1.17 (1.49)	1.14 (1.50)	1.07	1.06
V / V_{design}	1.00 (0.95)	1.01 (0.99)	1.04 (1.12)	1.08 (1.11)	0.97	1.04
$R_5 /R_{5, design}$	0.88 (0.91)	0.88 (0.92)	0.92 (1.07)	0.93 (1.08)	0.81	0.81

Table 5 gives 84th fractile values of the normalized peak tension forces in the braces as well as peak base shear forces and reactions R_5. The latter two parameters are normalized to the values used in design, as described earlier. Gravity load effects were removed from the R_5 values to allow direct comparison with seismic induced forces. Again, values in brackets for the BRB frames are for the bi-linear model and will be addressed next. As expected, higher BRB loads developed when L_c was shortened. However, the values are lower than anticipated for design (1.2 P_y), probably because the braces experienced only a few large plastic excursions (as in Figs. 7 & 8), thus mobilizing less isotropic strain hardening compared to test displacement protocols. At the 3rd floor, BRB loads did not reach the yield load, although ε_c exceeded the steel yield strain (0.19%). This may be due to the β and r values adopted in modeling, which could have led to too smooth transition between elastic and inelastic responses at small deformations. Tension load ratios in CBF braces exceeded unity, confirming the need to include strain hardening effects in the capacity design check for these structures. The base shear forces reached the values anticipated in design but the vertical reactions were slightly less than predicted, which can be attributed in part to the fact that not all braces developed their maximum forces at the same time over the three storeys.

Influence of brace modeling assumptions

Bi-linear models are more convenient for BRB modeling and they are more readily available in commercial analysis programs. As shown in Table 3, except at the top floor of the BRB-L frames, the use of a bi-linear model resulted in 5-20% underestimation of the M+SD storey drifts and core strain demand for both the long and short braces. Roof deformations and required roof separations were also under evaluated. Bi-linear models do not include Baushinger effects and, hence, exhibit initial elastic stiffness over a wider range of deformations. Upon yielding, they also have a constant stiffness, as opposed to actual BRB members that typically exhibit a flattening yielding response (see Fig. 6). For the BRB-L frames, the force demand predicted by the bi-linear model compares well with the results from the Ramberg-Osgoog formulation. For the BRB-S, the forces were overestimated as the strain demand experienced under the ground motions exceeded the 2% strain value that was used to set the stiffness upon brace yielding, and unrealistic forces are determined using that stiffness for values of ε_c beyond 2%.

CONCLUSIONS

The results of two sub-assemblage tests indicated that properly detailed and fabricated buckling restrained braces with core plates made from steel with enhanced toughness properties possess residual low-cycle fracture life capacity after the application of a qualifying seismic test protocol with cyclic core strain deformations of up to 3.5%. The design of a sample three-storey buildings showed that storey drifts can be reduced by specifying BRB members with shorter core dimensions, but this results in higher strain demand imposed on the brace cores. The example also showed that the design forces for capacity protected elements can be reduced significantly when adopting BRB frames compared to conventional CBF structures. Nonlinear dynamic analysis of the buildings studied confirmed these findings, indicating that low-rise BRB frames designed according to NBCC 2005 provisions with $R_d = 4.0$ can exhibit satisfactory seismic performance. The results clearly indicated, however, that the inelastic demand tends to concentrate at the bottom floor, resulting in core strain demand exceeding the design values, especially when short brace cores are specified. M+SD values of the computed-to-predicted ratios for the core strain were respectively 1.5 and 2.2 for the long and short core braces studied, and provisions must be made at the design stage for such higher demand.

The nonlinear dynamic analyses also demonstrated that conventional CBF structures can experience smaller lateral deformations compared to BRB frames, but similar drift amplification at the lower floor was observed and much larger forces were imposed on the surrounding structural elements. These forces can be well predicted for both the BRBF and the CBF systems using appropriate capacity design rules accounting for the expected sources of overstrength, including actual to nominal material property ratios, strain hardening response, and friction behavior for BRB members. When calibrating analytical model properties against BRB test results, caution should be exercised not to overestimate strain hardening contribution as the significant isotropic strain hardening that develops under typical test protocols may not be fully mobilized under actual seismic response. In this study, the deformation and strain demand were also found to be generally underestimated, while brace forces were overestimated for short core braces, when simple bi-linear modeling was adopted for reproducing BRB hysteretic response.

ACKNOWLEDMENTS

REFERENCES

1. Watanabe, A., Hitomi Y., Saeki, E., Wada, A., and Fujimoto, M. "Properties of Brace Encased in Buckling-Restraining Concrete and Steel Tube." Proc. 9th World Conference on Earthquake Engineering, Tokyo-Kyoto, Japan, Vol. IV: 719-724, 1988.

2. Saeki, E., Maeda, Y., Nakamura, H., Midorikawa, M., and Wada, A. "Experimental Study on Practical-Scale Unbonded Braces." J. Struct. Constr. Eng., AIJ, 1995; 476: 149-158 (In Japanese).

3. Maeda, Y., Nakata, Y., Iwata, M., and Wada, A. "Fatigue Properties of Axial-Yield type Hysteresis Dampers." J. Struct. and Constr. Eng., AIJ, 1998; 503: 109-115. (In Japanese)

4. Ko, E., Mole, A., Aiken, I., Tajirian, F., Rubel, Z., and Kimura, I. "Application of the Unbonded Brace in Medical Facilities." Proc. of the 7th U.S Nat. Conf. on Earthquake Eng., Boston, MA, Paper No. 514, 2002.

5. Iwata, M., Kato, T., and Wada, A. "Buckling-Restrained Braces as Hysteretic Dampers." Proc. STESSA 2000 Conf., 33-38, Montreal, Canada, August 2000. Rotterdam: Balkema, 2000.

6. Tsai, K.C. and Huang, Y.-C. "Experimental Responses of Large Scale Buckling Restrained Braced Frames." Report No. CEER R91-03, National Taiwan University, Tai-Pei, Taiwan, 2002.

7. SIE. "Tests on Nippon Steel Corporation Unbonded Braces – UC Davis Plant & Environmental Sciences Building." Report to Ove Arup & Partners California, Seismic Isolation Engineering, Inc., Oakland, CA, 1999.

8. Heidebrecht, A.C. "Overview of Seismic Provisions of the Proposed 2005 Edition of the National Building Code of Canada." Can. J. of Civ. Eng. 2003; 30(2): 241-254.

9. Bolduc. P. and Tremblay, R. "Experimental Study of the Seismic Behaviour of Steel Braces with Concrete Filled Tube and Double Steel Tube Buckling Restrained Mechanisms." Report No. EPM-GCS-2003-01, Dept. of Civil, Geological and Mining Eng., Ecole Polytechnique, Montreal, Canada, 2003.

10. Sabelli, R. "Research on Improving the Design and Analysis of Earthquake-Resistant Steel-Braced Frames." EERI/FEMA NEHRP Fellowship Report No. PF2000-9, Oakland, CA, 2001.

11. Chen, C.-C., Chen, S.-Y., and Liaw, J.-J. "Application of Low Yield Strength Steel on Controlled Plastification Ductile Concentrically Braced Frames." Can. J. of Civ. Eng. 2001; 28(5): 823-836.

12. CSA. "Limit states design of steel structures, CSA-S16-01." Canadian Standards Association, Rexdale, ON, 2001.

13. Mitchell, D., Tremblay, R., Karacabeyli, E., Paultre, P., Saatcioglu, M., and Anderson, D. "Seismic Force Modification Factors for the Proposed 2005 NBCC." Can. J. of Civ. Eng. 2003; 30(2): 308-327.

14. Tremblay, R. "Inelastic Seismic Response of Bracing Members." J. of Const. Steel Research 2002; 58: 665-701.

15. Carr, A.J. "RUAOMOKO, Inelastic Dynamic Analysis Program." Dept. of Civil Eng., University of Canterbury, NZ, 2002.

16. Nakashima, M., Akazawa, T., and Tsuji, B. "Strain-hardening behavior of shear panels made of low-yield steel. II: Model." ASCE Journal of Structural Engineering 1995; 121(12):1750-1757.

17. Prakash V, Powell GH. "DRAIN-2DX, DRAIN-3DX and DRAIN-BUILDING: Base program design documentation." Report UCB/SEMM-93/16, Department of Civil Engineering, University of California, Berkeley, Ca, 1993.

18. Ikeda, K. and Mahin, S.A. "A Refined Physical Theory Model for Predicting the Seismic Behavior of Braced Steel Frames." Report No. UCB/EERC-84/12, College of Eng., University of California, Berkely, CA, 1984.

19. Poncet, L. and Tremblay, R. "Seismic Performance of Multi-Storey Concentrically Braced Steel Frames with Mass Irregularity." Proc. 13th World Conference on Earthquake Engineering, Vancouver, Canada, Paper No. 2896, 2004.